Power Loss Analysis with High Primary Current in Magnetic Energy Harvesters

Jinyeong Moon, Steven B. Leeb
Department of Electrical Engineering and Computer Science
Massachusetts Institute of Technology
Cambridge, MA 02139, USA

***Abstract*—This paper presents an analysis of a magnetic energy harvester operating from a high power primary device with substantial current consumption. The existing 'transfer window alignment (TWA)' technique that can significantly boost the amount of harvested power from magnetic fields is revisited with a high primary current scenario, revealing that any shifting of the transfer window from passive rectification can be suboptimal once the primary side current goes beyond a certain level. This is caused by undesirable development of flux due to parasitic elements in the circuits. A new model to predict such an issue is first derived, and its simulation results are provided. The estimation of the critical level in the primary side current is explored, and the optimal strategy of a magnetic energy harvester that operates with a wide range of primary current is discussed.**

***Index Terms*—Magnetic Energy Harvester, Nonlinear Transformer, Transfer Window, TWA, Magnetic Saturation**

I. Introduction

Magnetic energy harvesting offers an excellent opportunity for self-powered sensors. Energy extraction from magnetic fields is reliable, unlike wind [1], [2], vibration [3], [4], temperature [5], or solar [6], since magnetic energy harvesting does not depend on environmental opportunities for energy harvesting. Furthermore, the level of energy extraction can be precisely predicted as well. Magnetic energy harvesting also provides relatively high energy density per physical volume compared to other existing technologies [7], [8]. The maximum harvestable power density of magnetic energy harvesting can reach $4\,\mathrm{mW}$ per $1\,\mathrm{cm}^3$ core volume and per $1\,\mathrm{A_{RMS}}$ primary current. To get a sense of how much volume is required for a sensor node, an extremely low power sensor example illustrated in [9] can be considered. This self-powered sensor node has a core volume of $2.9\,\mathrm{cm}^3$ to perform sensor data collection and wireless communication that consume $8\,\mathrm{mW}$ in total. The harvester extracts energy from magnetic fields generated by the primary side current of $0.7\,\mathrm{A_{RMS}}$. As the level of power harvest is proportional to the level of primary side current, a device with high primary current, e.g., a motor, can easily supply hundreds of mW (or even several W) with the same small core, which is mostly sufficient for a sensor application. The motor would only require tens of ampere.

One complication is that the magnetic core is periodically driven to magnetic saturation for maximum energy extraction [10], [11]. Magnetic saturation involves the nonlinear B-H curve of the core material and Maxwell's equations as well as external circuit constraints, making an accurate analysis a difficult job [10]. However, a "transfer window" introduced in [10] gives an insight on how magnetic saturation affects circuit operations and how to estimate in the first order the level of power harvest in the presence of magnetic saturation.

Based on the concept of the transfer window, methods to enhance power harvest are introduced in [11]. The transfer window alignment (TWA) method manipulates the location of the transfer window in an operating cycle, increasing the average current (hence power) it receives. The flux-shaping capacitor (FSC) method lengthens the transfer window by manipulating the rate that the flux is accumulated in the core. Both methods can be very effective, compared to the base case, i.e., passive rectification, making faster activation of a sensor node or a higher sensor count possible. Between these two methods, the TWA method has been our default enhancement to develop a magnetic energy harvester because of a minimal increase in physical volume and adaptability to a wider range of operating currents without special hardware.

However, our finding in this paper is that there is a critical drawback in the TWA method if a very high power primary side is accompanied. A second order effect that has been ignored in the most fundamental flux balance equation in [11] emerges as a severe limitation. A brief introduction to magnetic energy harvesting and the TWA method will be presented first. The new flux balance model will be introduced to incorporate this issue. Then, power loss due to high primary side current and the TWA method will be analyzed, and design guidelines to incorporate this issue will be presented.

II. Background

A. Magnetic Energy Harvesting

When a primary device is operating and conducting a current, magnetic fields are generated around a wire that carries the current. If an ungapped toroidal magnetic core is placed with a single winding of the primary side going through its center, the magnetic field (H) can be translated to the magnetic flux density (B) based on the B-H curve of the material that the core is consisted of. With flux area integration and time differentiation, B translates to the voltage developed across the two terminals of the core windings. If a load exists, an electric current required by the load is drawn from the core. Since the current is subject to the developed voltage across the core, power is harvested. This type of magnetic energy

978-1-4673-6847-6/15/$31.00 ©2015 IEEE

TABLE I
CORE PARAMETERS - VAC 500F W380

B_{SAT}	1.190 T
$P_{\text{LOSS-MAX}}$	0.125 mW
α	2.2
Outer Radius (r_{OD})	12.25 mm
Inner Radius (r_{ID})	8.25 mm
Height (h)	9 mm
Flux Area (A_{CORE})	3.6×10^{-5} m^2

harvesting purely depends on magnetic fields from the primary side without any permanent magnet or vibration associated. The amount of energy extraction given the size of the core can be reasonable for self-powered sensor nodes, facilitating easier deployment of magnetic energy harvesters. However, this type of energy harvesting has a problematic issue in terms of computation and circuit interpretation due to magnetic saturation.

B. Magnetic Saturation and Transfer Window

Though the accurate modeling of magnetic saturation requires a numerical solver, as discussed in [10], its qualitative properties with respect to circuit operations can be described with a few principles.

An amorphous nanocrystalline core (Vitroperm 500F W380 by VAC) is chosen as it exhibits an extremely high initial magnetic permeability with very low hysteresis loss. The configuration of the core is identical to a current transformer, and the core can be thought as a current source with highly nonlinear waveforms and bilateral signs. A rectifier is used to rectify this current, and the extracted energy is stored in the form of electric charges in a supercapacitor. Due to extremely high capacitance, the supercapacitor can be considered as a constant voltage load in the scope of $50-60$ Hz line frequency for the core. A high initial permeability – with a relative permeability on the order of hundreds of thousands as discussed in [9] – is essential for developing a sufficient voltage across the two terminals of the core as the core acts as a current source and it should be able to drive the rectifier. The parameters of the core are listed in Table. I. Note that α and $P_{\text{LOSS-MAX}}$ are calculated as defined in [10].

As the core enters magnetic saturation, the operating point of the B-H curve is at the 'flat' tail side, making $\partial B/\partial H$ (and $\partial B/\partial t$ as well) close to zero. Therefore, the effective voltage across the core (hence the shunt impedance of the core) is practically zero. As the configuration of the core is identical to a current transformer with $N:1$ ratio, magnetic saturation is identical to an internal short-circuiting path in the secondary side, so the entire secondary transformer current will return to the primary side without being delivered to the secondary load, harvesting zero power. In other words, magnetic energy extraction only happens during when the core is not saturated. The magnetic permeability of the core plays a vital role in transferring power as it directly increases the impedance of core when the core is not saturated, ensuring most of the current flows into the secondary load.

The term "transfer window" is defined to reflect this duration for which the power can be extracted from the secondary side. In the first order, the length of the transfer window can be estimated by equating the flux developed by voltage of the load in a half cycle to the maximally allowed flux for the core in a half cycle. The reason a half cycle is used is because of the rectifier to eliminate the bilateral signs of the transformer current before storing charges to the supercapacitor. Assuming a constant voltage load for the magnetic energy harvester, i.e., the supercapacitor charged to V_{LOAD}, the accumulated flux due to the load voltage over a half cycle is simply $V_{\text{LOAD}} \times t_{\text{SAT}}$, where t_{SAT} indicates the length of the transfer window. During this half cycle, B swings from one end to the other if the core enters saturation, for example, $-B_{\text{SAT}}$ to $+B_{\text{SAT}}$, where B_{SAT} refers to the saturation magnetic flux density. Therefore, the flux equality is:

$$V_{\text{LOAD}} \cdot t_{\text{SAT}} = 2\, B_{\text{SAT}} \cdot A_{\text{CORE}} \cdot N \tag{1}$$

And, the estimation of t_{SAT} is:

$$t_{\text{SAT}} = \frac{2\, B_{\text{SAT}} \cdot A_{\text{CORE}} \cdot N}{V_{\text{LOAD}}} \tag{2}$$

Here, denoted as A_{CORE} and N are the flux area and the number of windings in the secondary side of the core, respectively. Note that the equations above are only applicable to cases with constant voltage loads. If the load is not a constant voltage, then an explicit expression for t_{SAT} as in (2) will not be available in most of the cases.

C. The Transfer Window Alignment (TWA) Method

The transfer window alignment (TWA) method is to connect the load to the core such that the middle of the transfer window is precisely aligned with the peak of the primary sinusoidal current. It utilizes the fact that the level of the load voltage is an independent design variable from parameters of the primary side. It also relies on the fact that t_{SAT} does not contain any primary side variable as shown in (2). As soon as the load is connected to the core for a duration that is t_{SAT} long, the core goes into saturation, regardless of the location of the transfer window. By aligning the centers of the transfer window and the sinusoid, the average current that can be delivered to the load for a duration that is t_{SAT} long is maximized with the TWA method compared to the case with passive rectification. Since power harvest is the average current multiplied by the load voltage, which is constant, power harvest is directly enhanced. Though this is based on the qualitative reasoning with the first order approximation, the tendency matches well with the experiment as shown in [11]. Unlike the flux-shaping capacitor (FSC) method, which is also discussed as a means of enhancement in [11], the TWA method does not require a bank of passive elements, e.g., capacitors, for optimizing energy extraction. With the TWA method, the enhancement in energy extraction is achieved by more complex control with little overhead in physical complexity. Since the control can be easily integrated

into the existing microcontroller of a sensor suite, it is a very efficient enhancement for magnetic energy harvesters. However, the performance of the TWA method deteriorates at higher levels of the primary side current. In the subsequent sections, the drawbacks and limitations of the TWA method will be explored, starting with nonidealities in the flux balance model.

III. Power Loss Analysis

A. Limitation of the Simplest Flux Model

The equation (1) is based on the most fundamental flux equality until saturation. This first order linear equation can be deemed true as long as there is no other significant voltage drops across two terminals of the magnetic core except for the constant voltage load seen by the core. There are many nonideal elements that can cause deviations from this relationship with different levels of impact. An example is on-resistance of a switch. Whenever there exists a current, a voltage is developed across the on-resistance, stressing the core with additional flux. Assuming $100\,\mathrm{m\Omega}$ for simplicity, the on-resistance of a switch develops a peak voltage of $70.71\,\mathrm{mV}$ with a secondary current surge of $0.5\,\mathrm{A_{RMS}}$. Compared to the nominal constant voltage load of $4\,\mathrm{V}$ for instance, $70.71\,\mathrm{mV}$ from the on-resistance of a switch is fairly negligible. Furthermore, the secondary current of $0.5\,\mathrm{A_{RMS}}$ implies a $12\,\mathrm{kW}$ ($120\,\mathrm{V_{RMS}}$-$100\,\mathrm{A_{RMS}}$) device in the primary side with the windings of $N = 200$, which is a reasonable number of windings for a magnetic energy harvester. Therefore, many applications with similar or lower power ratings can neglect the effects of the on-resistance from the switches.

The example of on-resistance might sound assuring, but in essence, it is also clearly hinting at cases that this flux balance relationship will definitely fail to explain. One troublesome case is when there is a faulty component, for example, a failing diode with a high voltage drop. Also, a primary device that dissipates much higher than $12\,\mathrm{kW}$ will definitely cause a severe deviation from the given flux equality. Similarly, any resistance that is much higher than the on-resistance of a switch, for example, insufficiently thin wire, will cause a significant deviation even at the same or lower primary power levels. All of these cases will accumulate additional flux that is comparable in magnitude to the flux development of the load voltage, raising a need for a more accurate model for the flux balance. In fact, besides faulty circuit components which cannot be predicted at the design phase, the main issue due to a high primary side current arises from DC wire resistance of the windings. This will be explored in the next subsection, and the flux balance model will be expanded to include this secondary effect.

Note that such a deviation is caused by significant flux accumulation due to various elements, not only limited to higher primary currents. However, any significant flux accumulation in parasitic elements can be explained with the approach taken in this paper with higher primary power along with a scaled load voltage. Therefore, the analysis onward will consider the higher primary power case only for a simpler illustration.

B. New Flux Model

Assume secondary windings of 200 with a wire gauge of AWG30 and the same core parameters as described in Table. I. If it is a copper wire, the resistance of the wire is approximately $14\,\mathrm{m\Omega}$ per each turn that is approximately $4\,\mathrm{cm}$ for this magnetic core. This yields $2.8\,\Omega$ for 200 turns. This is an order of magnitude larger than on-resistance of a switch. When combined with the secondary current of $0.5\,\mathrm{A_{RMS}}$, voltage developed due to the DC resistance of the wire reaches $2\,\mathrm{V}$, which is directly comparable to the load voltage. Therefore, the flux accumulation from the wire resistance and the load voltage must be accounted together. A realistic modification to the flux equality leads to the following general equation:

$$\begin{aligned} &V_{\mathrm{LOAD}} \cdot (t_2 - t_1) + R_{\mathrm{DC}} \cdot \int_{t_0}^{t_2} \frac{I_{\mathrm{P}}}{N} \sin(\omega\,(t - t_0))\ \mathrm{d}t \\ &= \ 2\,B_{\mathrm{SAT}} \cdot A_{\mathrm{CORE}} \cdot N \end{aligned} \tag{3}$$

Denoted as t_0 is the most recent zero crossing point of the primary current. The start and the end time points of the transfer window are defined as t_1 and t_2. The angular frequency of the primary sinusoid is denoted as ω, and the amplitude of the primary side current is denoted as I_{P}. The DC resistance of the windings is denoted as R_{DC}. Essentially, the connection between the core and the constant voltage load will be made from $t = t_1$ to $t = t_2$, which is the transfer window. The magnetic core will enter saturation after $t = t_2$. Even though the transfer window starts from $t = t_1$, the voltage developed by the wire resistance must be accounted from the zero crossing of the transformer current to saturation, resulting in undesirable flux development. In practice, any other resistive component in flux development can be absorbed into R_{DC}. Similarly, any voltage component that contributes to faster saturation can be absorbed into V_{LOAD} with a proper scaling as well. In the next subsections, implications of the new flux balance model in existing harvesting methods will be discussed.

C. New Flux Model with Passive Rectification

Passive rectification can be represented by (3) if t_1 is set to t_0, which means the transfer window is initiated at the zero crossing of the primary side current. In this case, the flux equality can be simplified with the notion of the transfer window:

$$\begin{aligned} &V_{\mathrm{LOAD}} \cdot t_{\mathrm{SAT}} + \frac{R_{\mathrm{DC}}\, I_{\mathrm{P}}}{\omega\, N} \left[1 - \cos\left(\omega\, t_{\mathrm{SAT}}\right)\right] \\ &= \ 2\,B_{\mathrm{SAT}} \cdot A_{\mathrm{CORE}} \cdot N \end{aligned} \tag{4}$$

Here, t_{SAT} denotes the length of the transfer window. Since the right hand side of (4) is a physical constant once the core parameters are decided, any amount that the R_{DC} part develops results in a smaller amount for the V_{LOAD} part, hence a shorter t_{SAT}. In the same sense, if the R_{DC} part is negligible, for example, very low wire resistance or very low operating current, this equation approaches (1). After t_{SAT} is numerically obtained from (4), as an explicit solution is not available due

to the form of the equation, the actual harvested power in the case of passive rectification can be estimated by:

$$\begin{aligned} P_{\text{passive}} &= \frac{\omega}{\pi}\int_0^{t_{\text{SAT}}} V_{\text{LOAD}}\cdot\frac{I_{\text{P}}}{N}\sin(\omega\,t)\;\mathrm{d}t \\ &= \frac{V_{\text{LOAD}}\cdot I_{\text{P}}}{\pi\,N}\cdot[1-\cos\left(\omega\,t_{\text{SAT}}\right)] \end{aligned} \tag{5}$$

In passive rectification, the modified flux equality affects the calculation of t_{SAT}, and t_{SAT} is always lower than the ideal prediction. Since $[1-\cos(\omega\,t_{\text{SAT}})]$ also decreases as t_{SAT} decreases, lower power harvest is expected.

D. New Flux Model with the TWA method

Using the general equation (3), the TWA method can be represented by placing t_1 and t_2 with a symmetry around the peak of the primary sinusoid, i.e., $t_1 = T/4 - t_{\text{SAT}}/2$ and $t_2 = T/4 + t_{\text{SAT}}/2$, where T denotes the period of the primary sinusoid. The zero crossing of the primary side current (t_0) is no longer the same as t_1. In this case, with the notion of the transfer window, the general flux equation simplifies to:

$$\begin{aligned} &V_{\text{LOAD}}\cdot t_{\text{SAT}} + \frac{R_{\text{DC}}\,I_{\text{P}}}{\omega\,N}\left[1+\sin\left(\frac{\omega\,t_{\text{SAT}}}{2}\right)\right] \\ &= \;2\,B_{\text{SAT}}\cdot A_{\text{CORE}}\cdot N \end{aligned} \tag{6}$$

The form of the equation (6) is somewhat similar to that of (4) in that the equality also approaches (1) if the flux accumulation from the resistive part is negligible, and that any parasitic amount that the R_{DC} part develops directly decreases t_{SAT}. Specifically, if the primary side current increases, both (4) and (6) will result in shorter transfer windows as the weight toward the wire resistance increases. However, the behavior of (6) much differs from passive rectification if the parasitic term dominates the flux equality, causing a very small t_{SAT}. The fundamental difference is that the equation of passive rectification will not allow t_{SAT} to be zero while the equation (6) allows t_{SAT} to be zero in the TWA method. Zero t_{SAT} in the TWA method physically implies an extreme case where the core gets saturated even before the transfer window begins, resulting in zero power harvest. The DC resistance in the TWA case generates the entirety of the allowed amount of flux accumulation during when the core is supposed to be shorted to delay the transfer window, and the core gets saturated without ever connecting the load voltage to the core for power harvest. For the case of passive rectification, t_{SAT} physically cannot be zero because as soon as the core is recovered from magnetic saturation the wire and the load receive the same secondary transformer current and develop the flux at the same time for the same duration. Whether the window is extremely short or not depending upon the primary current and load voltage, this ensures nonzero t_{SAT} and nonzero power flow into the load before the core is again saturated.

With the advanced model equation comes a very important change in the analysis. Unlike the analysis done in the TWA section of [11], t_{SAT} is no longer independent of the primary side current. The TWA method originally maximizes energy harvesting by placing the transfer window at its optimal position, using independence of the transfer window from the primary side, as shown in (2). However, according to the more realistic flux equality (6), the position of the transfer window actually affects the length of the transfer window. Environment variables, e.g., frequency, now have different impacts on the length of the transfer window coupled with their dependency on the primary side as well. As a secondary effect, the modified equation also complicates the calculation since it cannot provide an explicit solution like (2). Note that the R_{DC} parts in the new flux equations of both passive rectification and the TWA method are actually independent of N due to the fact that R_{DC} itself is also proportional to N (multiplied by the unit resistance per turn).

In the original flux equality (1), doubling N means doubling t_{SAT}. In a physical sense, the saturation flux linkage is doubled, and the increased amount is solely consumed by the load voltage. Therefore, the core stays out of saturation exactly twice as longer. However, it does not mean that the power harvest will double, because the winding ratio is changed to $1:2N$ (the transformer current in the secondary side is halved). In fact, in the TWA method, J, which is a direct knob to control the level of power harvest and should be lowered to provide higher power harvest, is proportional to N/V_{LOAD}. Therefore, increasing only N actually results in lower energy extraction. A realistic design will always match V_{LOAD} such that J remains constant at least. A simulation result to validate these points will be presented shortly.

With the modified flux equality (6), however, doubling only N results in more than doubling t_{SAT}. This is because the right hand side – saturation flux linkage – is exactly doubled whereas the coefficients on the left hand side do not follow fast enough. To be specific, in passive rectification with (4), it can be shown that $1-\cos(\omega\cdot 2\,t_{\text{SAT}})$ is always smaller than $2\,[1-\cos\left(\omega\,t_{\text{SAT}}\right)]$. Therefore, doubling t_{SAT} on the left hand side still falls short compared to the right hand side with $2\,N$. Similarly in the TWA case with (6), it can be shown that $1+\sin\left(\frac{\omega\cdot 2\,t_{\text{SAT}}}{2}\right)$ is always smaller than $2\cdot\left[1+\sin\left(\frac{\omega\,t_{\text{SAT}}}{2}\right)\right]$. So in both scenarios, the left hand sides must be compensated with longer t_{SAT} to maintain the equality.

In practical situations where V_{LOAD} is also doubled to match J, the V_{LOAD} part on the left hand side is doubled and the total flux linkage on the right hand side is also doubled. However, the R_{DC} part on the left hand side remains rather constant regardless of changes in environmental variables. Therefore, the left hand side is not still sufficient to match the right hand side. Again, t_{SAT} has to be increased for the equality. As a result, the same J with higher N and higher V_{LOAD} performs better in energy extraction. A physical interpretation is simple: distributing the allowable saturation flux with more weight on the load voltage than the wire loss leads to higher power harvest. Since the same J with higher N yields a better result, high power primary cases should employ this approach for their designs. Fig. 1 illustrates the simulation results with different J and N combinations with the TWA method. Simulation results are obtained by LTSpice with the circuit model introduced

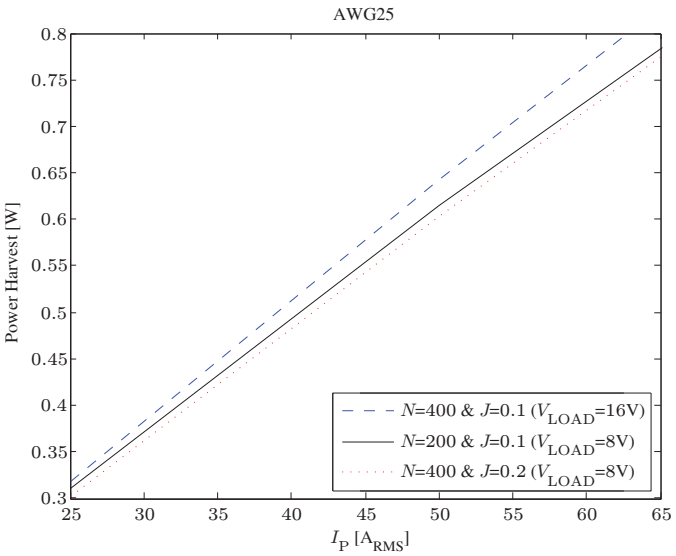

Fig. 1. Power harvest comparison with the same N or the same J under high power primary condition

in [11] and the core parameters given in Table. I. This is to illustrate realistic impacts of J, N, and V_{LOAD} and their differences on power harvest in detail in high power primary cases. It can be verified that increasing only N (with the same V_{LOAD}) is actually worse in power harvest (solid line vs. dotted line). Also, with the same J, the case with higher N and higher V_{LOAD} harvests more power according to the modified flux equality (dashed line vs. solid line). For the simulations, the wire gauge of AWG25 is used. Note that the difference between the dashed line and the solid line (the same J with different Ns) becomes larger as higher primary power levels put more weight toward the R_{DC} part in the flux balance. With the proposed flux balance model, these impacts can be hand-calculated as well, though it will be less accurate than numerical simulations. The accuracy of the modified flux model will be presented in the next subsection.

To summarize, the new flux equality affects the calculation of t_{SAT} in the TWA method as in passive rectification, but it includes the possibility of zero t_{SAT} unlike the case of passive rectification. Further delving into the TWA method, the new model presents that the same Js in the TWA method can yield different levels of power harvest due to different Ns, which change the level of the secondary transformer current and the amount of flux accumulation in parasitic elements.

E. Performance of the New Flux Model

The new flux balance model for passive rectification and the TWA method is tested against the simplest flux equality given in [11] (and also in (1)). The testing condition is set such that the parasitic flux accumulation takes up a significant portion in the flux balance. Table. II shows the improved accuracy on the estimations of t_{SAT} with the proposed flux equality model. Since the magnetic core with saturation is entwined with differential equations and nonlinear material properties, the proposed estimations as in (4) or (6) cannot be as accurate as the actual numerical circuit simulation. However, the modified flux balance model gives notably better estimations of t_{SAT} than the original flux equality. The most important part is that the crucial nonideality that drives zero t_{SAT} in the TWA method with high power primary cases can be properly considered during a design process to calculate the harvested power. Also can be verified is that in this high power primary cases passive rectification has a longer transfer window than the TWA method since the TWA method loses more flux to the resistive element before the load voltage is actually connected to the core. This is consistent with the zero t_{SAT} analysis. For the generation of Table. II, assumed are $\mathrm{freq} = 60\,\mathrm{Hz}$, $V_{\mathrm{LOAD}} = 4.0\,\mathrm{V}$, $N = 200$, $I_{\mathrm{P}} = 30\,\mathrm{A_{RMS}}$, and the wire gauge of AWG30.

TABLE II
ESTIMATIONS OF t_{SAT} WITH DIFFERENT FLUX EQUALITY MODELS

Flux Eq. Model	Passive Rect.	TWA Method
Existing [11]	4.284 ms	4.284 ms
Proposed	3.926 ms	3.641 ms
Simulation	3.836 ms	3.433 ms

In the next subsection, based on the proposed flux balance model, the practicality and efficiency of the TWA method will be explored, which will answer why any shifting of the transfer window from passive rectification results in suboptimal power harvest with high current primary cases.

F. The Effect of Higher Primary Current

Intuitively, a higher current in the primary side will generate stronger magnetic fields, increasing the amount of energy harvested from them. For passive rectification, this is true because the harvested power is proportional to $V_{\mathrm{LOAD}} \cdot I_{\mathrm{P}} \cdot [1 - \cos(\omega\, t_{\mathrm{SAT}})]$, as given in (5), and the rate at which I_{P} is increasing always overcomes the rate at which $[1 - \cos(\omega\, t_{\mathrm{SAT}})]$ is decreasing even with the proposed flux balance model. On the contrary for the TWA case, a higher current in the primary side does not necessarily mean higher power. It can greatly enhance power harvest for a certain range of I_{P}, but it has the clear extreme case where the entire allowable saturation flux is consumed by the wire resistance, which ends up with zero power harvest.

Initially from the zero primary current, energy extraction in the TWA method will be almost linear with the rise of I_{P} due to negligible voltage across the wire resistance. As the current in the primary side further increases, the wire resistance develops higher voltage across it and a deviation from the ideal case will grow larger. A thicker wire will sustain the near-ideal behavior longer than a thinner wire since the thicker wire will have assigned more flux accumulation toward the load voltage. The simulation results are provided in Fig. 2, illustrating an effect of wire thickness on energy extraction across a range of primary current levels. They all start as a linear function when

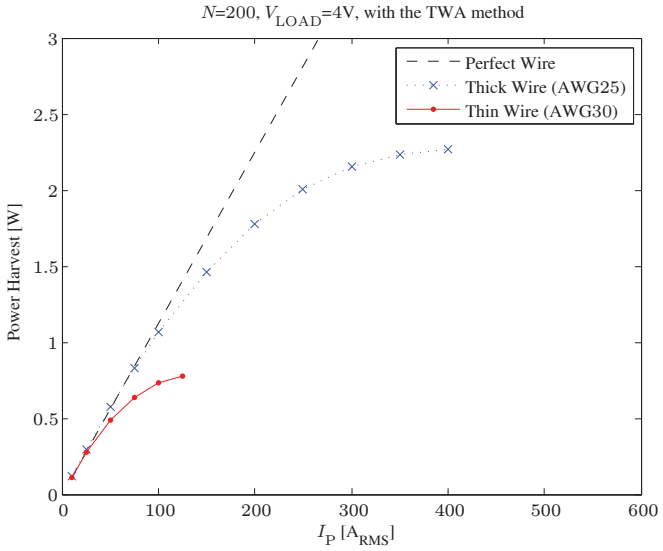

Fig. 2. Power harvest comparison with different DC wire loss under high power primary condition

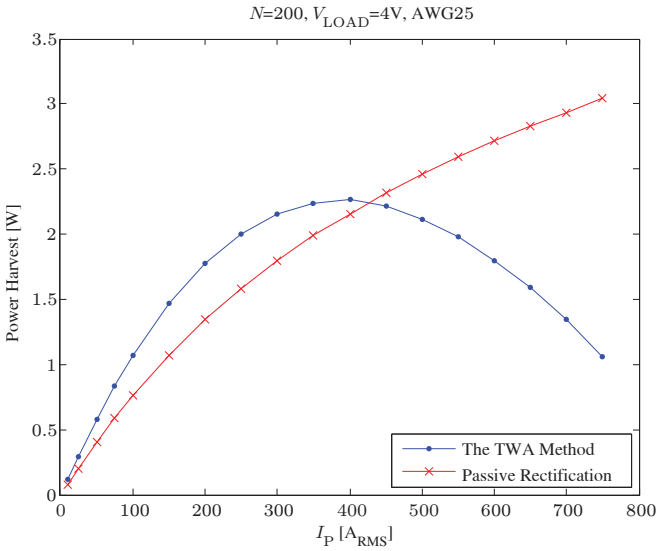

Fig. 3. Nonideal effects on the TWA method under high power primary condition

the primary side carries a lower current. As the current goes up, the voltage developed across the wire resistance causes deviation from the ideal wire case. Clearly, the thicker wire is closer to the ideal case as it can ensure a longer t_{SAT}. If the current range of the primary side is pre-determined, the wire gauge can be calculated based on how much deviation is allowed for the maximum power case. This will be described in the next section. Note that each curve in the figure is drawn up to the maximum power harvest point. After the maximum power harvest points, the losses in the transfer windows due to the wire resistances surpass the gains in power harvest with higher primary currents. The curves will eventually converge to zero as t_{SAT} becomes zero.

The TWA method enhances the amount of power harvested from the core compared to the base case with passive rectification, assuming low primary current levels. However, power harvest with the TWA method can decrease to zero with higher primary currents while passive rectification guarantees higher power harvest with higher primary currents. Therefore, the curves of harvested power using two methods will intersect. Using a much wider I_{P} range, the levels of energy extraction for both passive rectification and the TWA method are depicted in Fig. 3. This simulation result shows the aforementioned point where the passive rectification surpasses the TWA method, which occurs at $I_{\mathrm{P-critical}} = 425.4\,\mathrm{A_{RMS}}$. Denoting the lengths of the transfer windows in passive rectification and the TWA method as t_{SAT1} and t_{SAT2}, respectively, the point can be estimated by combining (4), (6), and the following equation that forces the same power level at the intersection.

$$\begin{aligned} &\frac{2}{T}\int_0^{t_{\mathrm{SAT1}}} V_{\mathrm{LOAD}}\cdot\frac{I_{\mathrm{P}}}{N}\sin(\omega\,t)\;\mathrm{d}t \\ &= \frac{2}{T}\int_{\frac{T}{4}-\frac{t_{\mathrm{SAT2}}}{2}}^{\frac{T}{4}+\frac{t_{\mathrm{SAT2}}}{2}} V_{\mathrm{LOAD}}\cdot\frac{I_{\mathrm{P}}}{N}\sin(\omega\,t)\;\mathrm{d}t \end{aligned} \tag{7}$$

When simplified, (7) becomes:

$$1-\cos(\omega\,t_{\mathrm{SAT1}}) = 2\sin\left(\frac{\omega\,t_{\mathrm{SAT2}}}{2}\right) \tag{8}$$

Note that since the solution of (4), (6), and (8) does not come in an explicit form, it has to be numerically solved. The intersection of the two curves of Fig. 3 can be estimated to be $I_{\mathrm{P-critical}} = 478.29\,\mathrm{A_{RMS}}$ by solving three equations. Once again, this differs from the accurate circuit simulation of $425.4\,\mathrm{A_{RMS}}$, but gives a fairly good estimate for quick design targets as a first order hand calculation. After this critical level, there is no gain by using the TWA method anymore, and the best energy extraction will be again by setting zero shift for the transfer window from passive rectification because it minimizes the flux loss in other elements than the load voltage.

IV. Design for Lower Power Loss

A. Wire Considerations for Lower Power Loss

For a given primary current profile, the thickness of the windings can be increased to lower the power loss due to the resistive element in the flux balance. A tradeoff exists as the thickness of the windings can reduce the resistance, but also reduce the center window area of the core that the primary wire goes through. To provide a way to calculate wire thickness, the following two equations can be set up:

$$p = \frac{\dfrac{R_{\mathrm{DC}}\,I_{\mathrm{P}}}{\omega\,N}\left[1+\sin\left(\dfrac{\omega\,t_{\mathrm{SAT}}}{2}\right)\right]}{2\,B_{\mathrm{SAT}}\cdot A_{\mathrm{CORE}}\cdot N} \tag{9}$$

and

$$(1-p) = \frac{V_{\mathrm{LOAD}}\cdot t_{\mathrm{SAT}}}{2\,B_{\mathrm{SAT}}\cdot A_{\mathrm{CORE}}\cdot N} \tag{10}$$

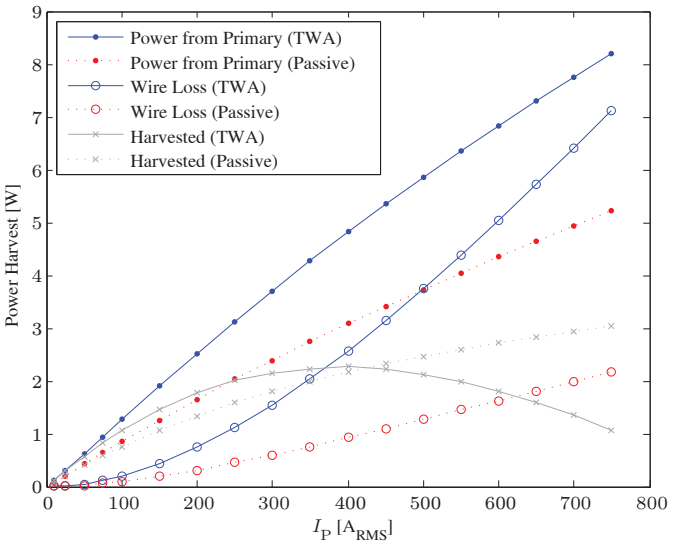

Fig. 4. Wire loss comparison between the TWA method and passive rectification

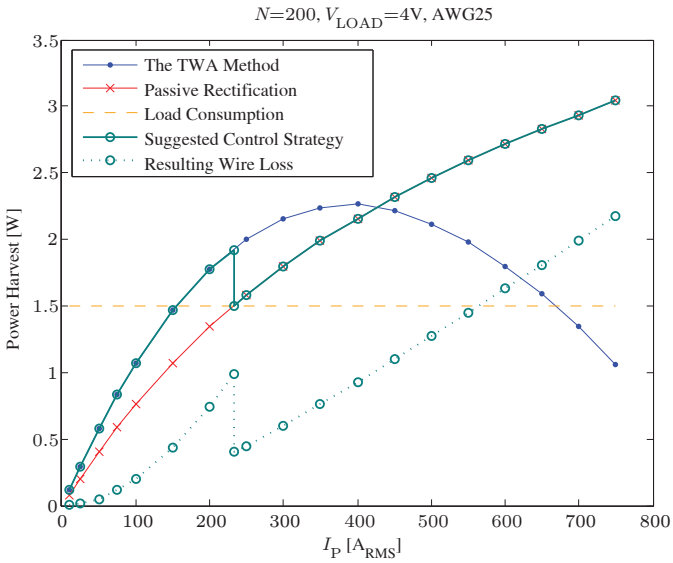

Fig. 5. Suggested control strategy and the resulting wire loss

Here, p represents the ratio of the flux accumulation due to the R_{DC} part in the flux balance to the total allowable flux accumulation. The rest of the allowed flux, $(1-p)$, is assigned to the V_{LOAD} part. Combining two equations can eliminate t_{SAT} and yield the following equation for the R_{DC} for a given I_{P}:

$$\frac{R_{\mathrm{DC}}}{N} = \frac{p \cdot 2\,\omega\, B_{\mathrm{SAT}}\, A_{\mathrm{CORE}}\, N}{I_{\mathrm{P}} \cdot \left[1 + \sin\left(\dfrac{(1-p)\,\omega\, B_{\mathrm{SAT}}\, A_{\mathrm{CORE}}\, N}{V_{\mathrm{LOAD}}}\right)\right]} \tag{11}$$

For example, allowing 10% for parasitic flux accumulation ($p = 0.1$), R_{DC}/N should be lower than $2.744\,\mathrm{m\Omega}$ (which gives $0.549\,\Omega$ for 200 turns), using the same core parameters as in Table. I, $V_{\mathrm{LOAD}} = 4\,\mathrm{V}$, and $I_{\mathrm{P}} = 100\,\mathrm{A_{RMS}}$. The per-turn resistance value and the size of the core indicate that the cross-sectional area of the wire must be larger than $0.244\,\mathrm{mm^2}$ as each turn is approximately $4\,\mathrm{cm}$ long in this example. The design decision will be then AWG23 for the wire. The remaining question is how to select p. One aspect is the allowable heat dissipation for the wire or the temperature limit of the harvester system as p is directly coupled with power loss in the wire. In our experiences, heat or temperature issue results in less conservative p, compared to the efforts to keep the level of power harvest and t_{SAT} not deviating too much from the ideal expectations. Our suggestion is to use $p = 10\%$ if the heat and temperature issues are verified to be secondary constraints.

If the core is already wound with a certain wire gauge without knowledge of the primary side, the maximum I_{P} that the constructed core can operate without being inefficient or incapable can be also calculated by swapping the positions of R_{DC}/N and I_{P} in (11).

B. Suggested Control Strategy

Assume a case where the level of the primary side current changes much over time, for example, periodic speed control of a motor. The TWA method and the FSC method can be useful for enhancing energy extraction, but the TWA method can be more efficient in terms of physical space and easier control with varying primary currents. One limitation is that the TWA method is only efficient when the primary side carries a relatively lower current, for example, $I_{\mathrm{P}} \leq 400\,\mathrm{A_{RMS}}$ in Fig. 3. The power electronic circuits must switch back to the passive mode after I_{P} reaches $I_{\mathrm{P-critical}}$ since the amount of harvested power gets smaller than passive rectification. Furthermore, more power is dissipated in the wire in the TWA method compared to the case with passive rectification, leading to unnecessary heat generation. Figure 4 illustrates the simulation results of wire losses in two cases. Assumed are $N = 200$, $V_{\mathrm{LOAD}} = 4\,\mathrm{V}$, and the wire gauge of AWG25. Two curves marked with solid dots illustrate the total power drawn from the primary side. The TWA method clearly extracts more power from the primary side. However, the wire loss curves, marked with hollow circles, show that the TWA method loses a significant portion of the extracted power from the primary side as I_{P} increases whereas the wire loss in passive rectification increases at a slower rate. To give a perspective, two curves from Fig. 3, the actual power harvested in the secondary side, are overlaid here, marked with 'x'. The wire loss in the TWA method surpasses the actual power harvest from the load even before $I_{\mathrm{P-critical}}$ occurs. It can be expected that as the harvested power with the TWA method approaches zero, the wire loss will be indistinguishable from the power extracted from the primary side.

Due to the drawbacks that the TWA method has, it might be realistic to switch the circuit mode before $I_{\mathrm{P-critical}}$ occurs or the wire loss dominates. The required condition is that the harvester operating with passive rectification can extract

more than the load power consumption of the sensor node, usually hundreds of mW for most of the sensor applications. It will benefit both the sensor node and the primary side by decreasing the heat generation and eliminating unnecessary power loss. The suggested control scheme is illustrated in Fig. 5 as a solid line with hollow circles. Here, the load power consumption with some margin, depicted as the dashed line, is set at $1.5\,\mathrm{W}$. The circuit that originally operates with the TWA method changes the mode to passive rectification when the level of the primary current is higher than the threshold, which is $233.07\,\mathrm{A_{RMS}}$ for this simulation. More dynamically, the control for the mode switch can be autonomous with the microcontroller. By detecting a positive change in voltage of the supercapacitor over a multiple of operating cycles, it can be verified that the TWA method generates more than what the load consumes. Once this is detected, passive rectification can be sparsely tried until a positive change in voltage of the supercapacitor is detected with passive rectification as well. With this dynamic approach, no preset of the threshold level in the primary current is required.

V. Conclusion

A new flux balance model has been introduced to incorporate the issue that occurs in the most fundamental flux equality [10], [11] when there is a significant flux loss due to parasitic elements. As a representative example of such a parasitic flux loss, DC wire resistance in a high power primary case was analyzed. The paper demonstrated why the original flux equality is insufficient for circuits with high primary current cases, and presented a new set of equations for more accurate analyses. The performance of the proposed model was proven to be more accurate than the existing flux balance model. Deviations in the levels of power harvest from ideal expectations were analyzed and the implications in the design optimization of the TWA method were explored with the new model. The most important points with the new flux model are that t_{SAT} is no longer independent of the primary side and that zero t_{SAT} is possible with the TWA method. This indicates that a higher primary current can actually result in lower power harvest under certain circumstances, and in extreme cases the core can never extract energy at all. The paper also expands this phenomenon to explain why any shifting of the transfer window from passive rectification results in suboptimal power harvest with high primary current levels. The paper presented a way to calculate the critical level in the primary current where the TWA method performs inferior to passive rectification. It also provided an equation to determine wire thickness given the primary current profile. The control strategy with a varying current level in the primary side is presented for better power harvest and lower power loss.

Acknowledgements

The authors gratefully acknowledge the support of the Kwanjeong Educational Foundation, the Office of Naval Research Structural Acoustics Program, and The Grainger Foundation.

References

[1] D. Porcarelli, D. Spenza, D. Brunelli, A. Cammarano, C. Petrioli, L. Benini, "Adaptive rectifier driven by power intake predictors for wind energy harvesting sensor networks," *IEEE J. Emerg. Sel. Topics Power Electron.*, vol. 3, no. 2, pp. 471-482, Jun. 2015.

[2] Y. Tan, S. Panda, "Self-autonomous wireless sensor nodes with wind energy harvesting for remote sensing of wind-driven wildfire spread," *IEEE Trans. Instrum. Meas.*, vol. 60, no. 4, pp. 1367-1377, Apr. 2011.

[3] S. Meninger, J. Mur-Miranda, R. Amirtharajah, A. Chandrakasan, and J. Lang, "Vibration-to-electric energy conversion," *IEEE Trans. Very Large Scale Integr. (VLSI) Syst.*, vol. 9, no. 1, pp. 64-76, Feb. 2001.

[4] G. Ottman, H. Hofmann, A. Bhatt, and G. Lesieutre, "Adaptive piezoelectric energy harvesting circuit for wireless remote power supply," *IEEE Trans. Power Electron.*, vol. 17, no. 5, pp. 669-676, Sep. 2002.

[5] I. Stark, "Thermal energy harevsting with thermo life," *IEEE Intl. Workshop on Wearable and Implantable Body Sensor Networks*, pp. 19-22, Apr. 2006.

[6] V. Raghunathan, A. Kansal, J. Hsu, J. Friedman, M. Srivastava, "Design considerations for solar energy harvesting wireless embedded systems," *IPSN 2005. Fourth International Symposium on*, pp. 457-462, Apr. 2005.

[7] M. Pinuela, P. Mitcheson, S. Lucyszyn, "Ambient RF energy harvesting in urban and semi-urban environments," *IEEE Trans. Microw. Theory Techn.*, vol. 61, no. 7, pp. 2715-2726, Jul. 2013

[8] S. Sudevalayam and P. Kulkarni, "Energy harvesting sensor nodes: survey and implications," *IEEE Commun. Surv. Tutorial*, vol. 13, no. 3, pp. 443-461, 2011.

[9] J. Moon, J. Donnal, J. Paris, S. Leeb, "VAMPIRE: self-powered sensor node capable of wireless transmission," *IEEE APEC*, Mar. 2013

[10] J. Moon, S. Leeb, "Analysis model for magnetic energy harvesters," *IEEE Trans. Power Electron.*, vol 30, no. 8, pp. 4302-4311, Aug. 2015

[11] J. Moon, S. Leeb, "Power electronic circuits for magnetic energy harvesters," *IEEE Trans. Power Electron.*, Dec. 2015